Applied Physics Express

LETTER • OPEN ACCESS

High-speed growth of thick high-purity β-Ga_2O_3 layers by low-pressure hot-wall metalorganic vapor phase epitaxy

OPEN ACCESS

Applied Physics Express 16, 095504 (2023) LETTER

https://doi.org/10.35848/1882-0786/acf8ae

High-speed growth of thick high-purity β-Ga_2O_3 layers by low-pressure hot-wall metalorganic vapor phase epitaxy

Junya Yoshinaga[1], Haruka Tozato[2], Takahito Okuyama[2], Shogo Sasaki[3], Guanxi Piao[1], Kazutada Ikenaga[1,2], Ken Goto[2], Yuzaburo Ban[4], and Yoshinao Kumagai[2,3*]

[1]TAIYO NIPPON SANSO CORPORATION, Tsukuba, Ibaraki 300-2611, Japan
[2]Department of Applied Chemistry, Tokyo University of Agriculture and Technology, Koganei, Tokyo 184-8588, Japan
[3]FLOuRISH Institute, Tokyo University of Agriculture and Technology, Koganei, Tokyo 184-8588, Japan
[4]TAIYO NIPPON SANSO CSE LTD., Kawasaki, Kanagawa 210-0861, Japan

*E-mail: 4470kuma@cc.tuat.ac.jp

Received August 25, 2023; revised September 5, 2023; accepted September 10, 2023; published online September 28, 2023

High-speed growth of thick, high-purity β-Ga_2O_3 homoepitaxial layers on (010) β-Ga_2O_3 substrates by low-pressure hot-wall metalorganic vapor phase epitaxy was investigated using trimethylgallium (TMGa) as the Ga precursor. When the reactor pressure was 2.4–3.4 kPa, the growth temperature was 1000 °C, and a high input VI/III (O/Ga) ratio was used, the growth rate of β-Ga_2O_3 could be increased linearly by increasing the TMGa supply rate. A thick layer was grown at a growth rate of 16.2 μm h^{-1} without twinning. Incorporated impurities were not detected, irrespective of the growth rate, demonstrating the promising nature of β-Ga_2O_3 growth using TMGa. © 2023 The Author(s). Published on behalf of The Japan Society of Applied Physics by IOP Publishing Ltd

Beta gallium oxide (β-Ga_2O_3) has attracted much attention as an ultra-wide-bandgap semiconductor for next-generation power devices because of its large bandgap energy of ~4.5 eV[1,2] and predicted large dielectric breakdown field strength of 7–8 MV cm^{-1}.[3,4] Taking advantage of the ability to produce single-crystal substrates with low dislocation densities from β-Ga_2O_3 bulk crystals grown by various melt methods,[5–7] researchers are actively developing various devices using homoepitaxial layers grown on them. Thick (~10 μm) *n*-type homoepitaxial (drift) layers with controlled carrier densities of approximately 10^{16} cm^{-3} are critical for the development of vertical devices.[8–13] Currently, such layers are grown exclusively by halide vapor phase epitaxy (HVPE),[14–16] which can grow β-Ga_2O_3 at high speeds.

On the other hand, rapid progress in β-Ga_2O_3 growth by metalorganic vapor phase epitaxy (MOVPE) has recently been reported.[17–20] This interest stems from the expectation that MOVPE not only can enable excellent controllability of the thickness of the β-Ga_2O_3 layers and the composition of $(Al_xGa_{1-x})_2O_3$ alloys but also has excellent mass production capabilities. High-purity β-Ga_2O_3 layers without carbon (C) contamination have been grown using triethylgallium (TEGa) and oxygen (O_2) as precursors and argon (Ar) as a carrier gas.[17–20] Some of the authors of the present work investigated the same system in combination with thermodynamic analysis and mass spectrometry.[21–23] They found that the key to growing homoepitaxial layers without C and hydrogen (H) contamination is the pyrolysis of TEGa into gaseous Ga and ethylene (C_2H_4) via a β-hydrogen elimination reaction[24] at low temperatures above 400 °C and the growth of β-Ga_2O_3 at high temperatures around 1000 °C to completely burn C_2H_4 to produce carbon dioxide (CO_2) and water (H_2O).[23] Several prototypes of Schottky barrier diodes and FETs using thin MOVPE-grown β-Ga_2O_3 layers have already been reported.[25–27] However, the growth rate of β-Ga_2O_3 using TEGa is low (~1 μm h^{-1} at most), which is not suitable for growing the thick drift layers required for vertical devices.

To increase the growth rate of β-Ga_2O_3, researchers have begun investigating MOVPE using trimethylgallium (TMGa), which has a much higher vapor pressure than TEGa.[28,29] However, the change of the growth conditions when TMGa is used compared to those when TEGa is used and whether the concentration of various impurities in the grown layer can be reduced have not been investigated. In the present study, we clarify the effect of the growth conditions of β-Ga_2O_3 layers using TMGa on the growth rate and the incorporation of various impurities, especially C, and demonstrate the high-speed growth of high-purity layers at speeds exceeding 16 μm h^{-1}.

A horizontal low-pressure hot-wall MOVPE reactor (TAIYO NIPPON SANSO, FR2000-OX) made of quartz glass, in which the mixing zone of the precursors (upstream) and the growth zone of β-Ga_2O_3 (downstream) are heated separately by a multizone electric furnace, was used. TMGa or TEGa was used as the Ga precursor, and pure O_2 was used as the oxygen precursor. The Ga and oxygen precursors were fed into the flow channel (10 mm high) at high linear velocities using a narrow-gap three-layered injection nozzle along with Ar carrier gas, which suppressed premature reactions before reaching the substrate; TMGa or TEGa was injected through the middle layer of the nozzle, and O_2 was injected through the upper and lower layers of the nozzle. The total gas flow rate was fixed at 8400 sccm. In the growth zone, a substrate holder, which can accommodate a substrate with a diameter as large as 2 inches and can be rotated, was placed parallel to the flow channel with the substrate surface facing down.

Two types of substrates were used: 2 inch diameter nominally (0001) sapphire (Orbray) and 10 × 15 mm^2 nominally (010) β-Ga_2O_3 (Novel Crystal Technology). After the substrate was placed in the holder, the reactor was evacuated to a pressure of 1.4–11.7 kPa. The mixing and growth zones were then heated to 920 and 1000 °C, respectively, in an Ar stream containing O_2. Subsequently, the TMGa or TEGa supply was started and the β-Ga_2O_3

growth was carried out for 1 h. After the growth, the supply of TMGa or TEGa was stopped and the substrate was cooled to room temperature.

The thickness of the β-Ga_2O_3 heteroepitaxial layers was evaluated by cross-sectional observation using scanning electron microscopy (SEM), while the thickness of the homoepitaxial layers was measured by Fourier transform infrared (FT-IR) spectroscopy. The concentrations of impurities were evaluated by secondary-ion mass spectrometry (SIMS). The surface morphology was observed using Nomarski differential interference contrast (NDIC) microscopy and atomic force microscopy (AFM). The crystal orientation and perfection of the grown layers were investigated by high-resolution X-ray diffraction (XRD) using a Cu $K\alpha_1$ beam.

An input VI/III (O/Ga) ratio suitable for MOVPE of β-Ga_2O_3 using TMGa or TEGa was first investigated. Figure 1 shows the in-plane distributions of the growth rate of ($\bar{2}01$)-oriented β-Ga_2O_3 grown on sapphire substrates without substrate rotation at a reactor pressure of 1.4 kPa, a TMGa or TEGa supply rate of 1.8×10^2 μmol min^{-1} (corresponding to an input partial pressure of 0.69 Pa), and input VI/III ratios of 97 to 1900. The bubbler settings were 4 °C and 101.0 kPa for TMGa and 30 °C and 101.0 kPa for TEGa. When TEGa was used, growth rates of $\sim$1 μm h^{-1} were achieved across the entire substrate at an input VI/III ratio of 97. By contrast, when growth was attempted using TMGa under the same conditions used for TEGa, no growth occurred. With TMGa, β-Ga_2O_3 growth was observed downstream of the substrate at the input VI/III ratio of 490 and growth occurred over the entire substrate at an average rate of 4.7 μm h^{-1} when the input VI/III ratio was 970. When the input VI/III ratio was 1900, the growth rate was slightly higher than when the input VI/III ratio was 970. These results indicate that the reaction between TMGa and O_2 occurs only at higher input VI/III ratios, i.e., under higher input partial pressures of O_2, than the reaction between TEGa and O_2. This might be related to the fact that highly reactive gaseous Ga is readily generated by a β-hydrogen elimination reaction when TEGa is used,[21,23,24] whereas no such decomposition mechanism is active when TMGa is used.[24]

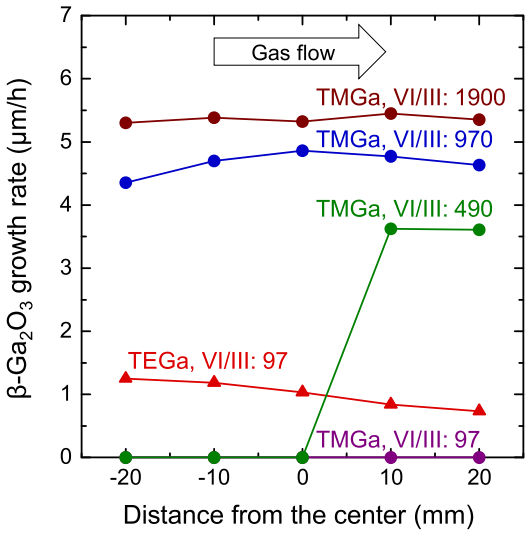

Fig. 1. Input VI/III ratio dependence of the in-plane distributions of growth rates of β-Ga_2O_3 at 1000 °C on 2 inch diameter (0001) sapphire substrates. The supply rate of TMGa or TEGa was fixed at 1.8×10^2 μmol min^{-1}, and the substrate was not rotated during the growth.

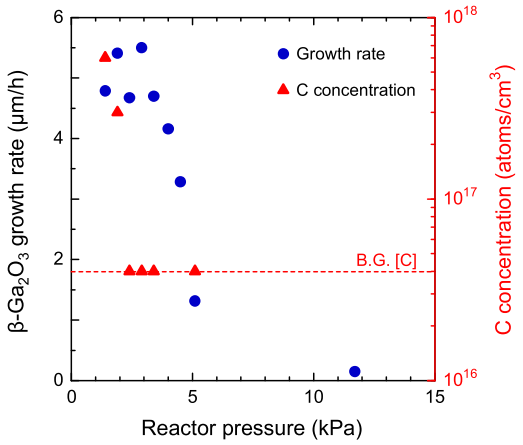

Fig. 2. Reactor pressure dependence of the growth rate and C concentration of ($\bar{2}01$) β-Ga_2O_3 heteroepitaxial layers grown on (0001) sapphire substrates using TMGa. The TMGa supply rate and input VI/III ratio were 1.8×10^2 μmol min^{-1} and 970, respectively. The dashed line indicates the B.G. level of C impurities.

Next, β-Ga_2O_3 layers were grown on sapphire substrates using TMGa by varying the reactor pressure. Figure 2 shows the reactor pressure dependence of the ($\bar{2}01$) β-Ga_2O_3 growth rate and the concentration of TMGa-derived C impurities in the grown layers under a fixed TMGa supply rate and input VI/III ratio of 1.8×10^2 μmol min^{-1} and 970, respectively. The growth rate of β-Ga_2O_3 was kept constant at $\sim$5 μm h^{-1} when the reactor pressure was between 1.4 and 3.4 kPa but decreased rapidly when the reactor pressure exceeded 3.4 kPa. This result is likely attributable to the reaction between TMGa and O_2 becoming more likely to occur when the reactor pressure increases, eventually leading to gas-phase reactions. On the other hand, the C concentration decreased rapidly with increasing reactor pressure and was less than the SIMS background (B.G.) level (4×10^{16} atoms cm^{-3}) at reactor pressures greater than 2.4 kPa. In the investigated reactor pressure range, the concentrations of other impurities, H, nitrogen (N), and

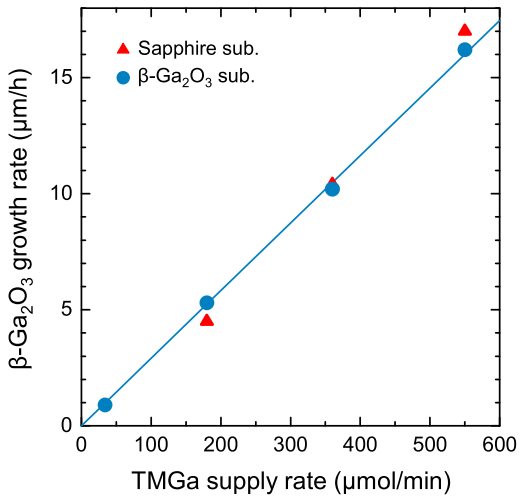

Fig. 3. TMGa supply rate dependence of the MOVPE growth rate of β-Ga_2O_3 layers on (0001) sapphire and (010) β-Ga_2O_3 substrates at a reactor pressure of 2.4 kPa. The solid line is a guide to the eye.

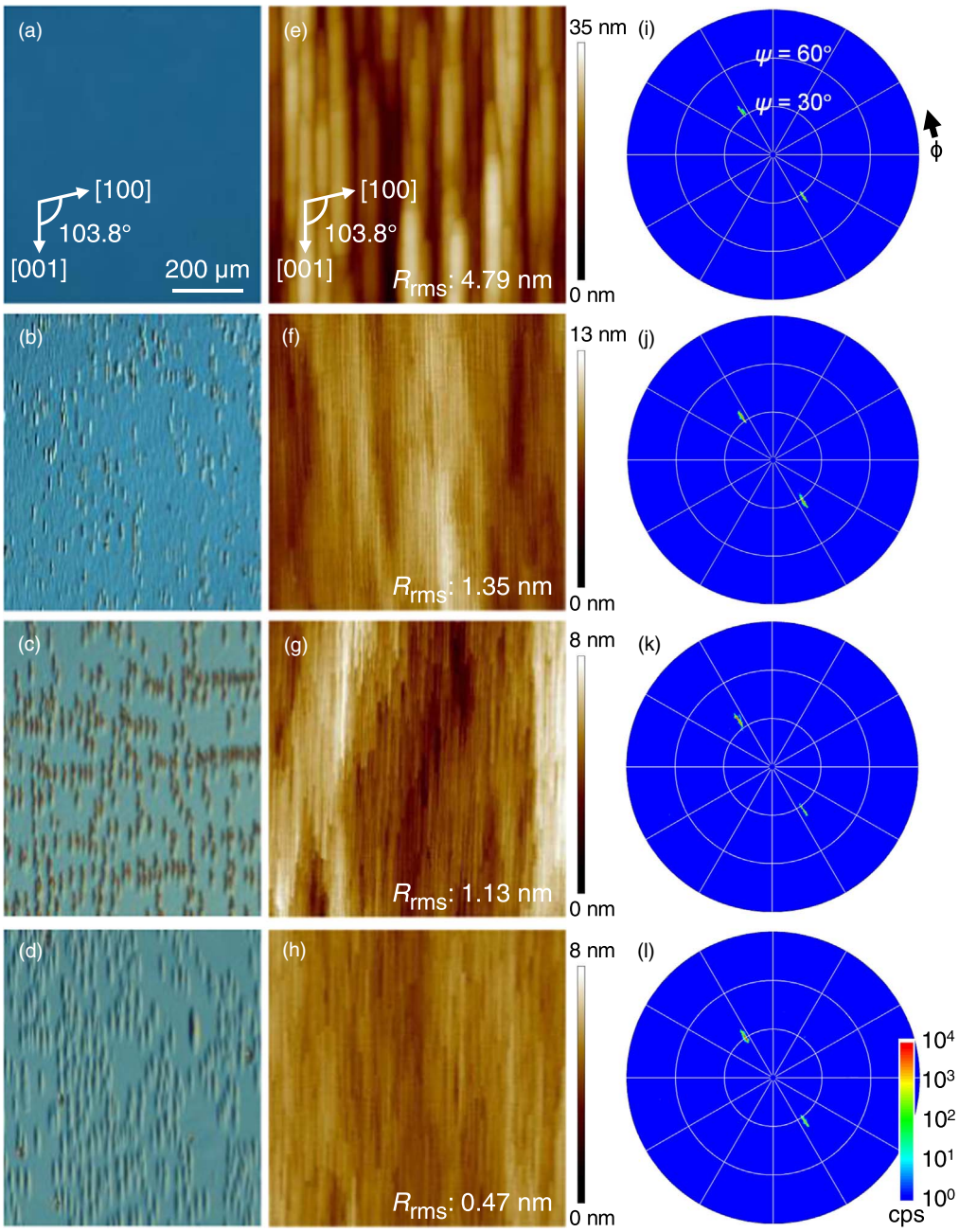

Fig. 4. (a)–(d) Surface NDIC microscopy images, (e)–(h) surface AFM images of 2 × 2 μm^2 scan areas, and (i)–(l) XRD {111} pole figures of homoepitaxial layers grown on (010) β-Ga_2O_3 substrates for 1 h at various TMGa supply rates [(a),(e),(i) 3.4 × 10^1, (b),(f),(j) 1.8 × 10^2, (c),(g),(k) 3.6 × 10^2, and (d),(h),(l) 5.5 × 10^2 μmol min^{-1}]. The R_{rms} value is shown in each AFM image. In the pole-figure measurements, ϕ is 0° when the incident azimuth of the X-ray is parallel to [00$\bar{1}$]; increasing ϕ corresponds to the clockwise rotation of the substrate.

silicon (Si), were below their respective B.G. levels (2 × 10^{17} atoms cm^{-3} for H, 2 × 10^{16} atoms cm^{-3} for N, and 1 × 10^{16} atoms cm^{-3} for Si) irrespective of the reactor pressure. These results show that increasing the reactor pressure not only promotes the reaction between TMGa and O_2 but also promotes combustion of C-containing gaseous species. Notably, the Si impurity concentration in the layers grown using TMGa was below the B.G. level, which was different from the high Si impurity concentration of 7 × 10^{17} atoms cm^{-3} in the layer grown using TEGa (i.e., the layer shown in Fig. 1). This result is speculatively attributed to the stabilization of the quartz glass reactor wall because the growth of β-Ga_2O_3 with TMGa uses a much higher input VI/III ratio (O_2 input) than the growth with TEGa. The aforementioned results clarify that high-purity β-Ga_2O_3 layers can be grown without a reduction in the growth rate by conducting growth in the reactor pressure range from 2.4 to 3.4 kPa.

Finally, the TMGa supply rate dependence of the growth rate of β-Ga_2O_3 on sapphire and β-Ga_2O_3 substrates was investigated at a reactor pressure of 2.4 kPa. Growth was performed with the substrate rotating at 1 rotation per minute. The TMGa supply rate was varied from 3.4 × 10^1 to 5.5 × 10^2 μmol min^{-1} and the input partial pressure of O_2 was fixed at 570 Pa (the resultant input VI/III ratio was 5300 to 330). The results are shown in Fig. 3. Although the input VI/III ratio decreased with increasing TMGa supply, the growth rate of β-Ga_2O_3 increased linearly (i.e., so-called mass-transportation-limited growth behavior was observed) and a high growth rate greater than 16 μm h^{-1}, comparable to the growth rate by HVPE,[14] was achieved. No difference was observed in the growth rate

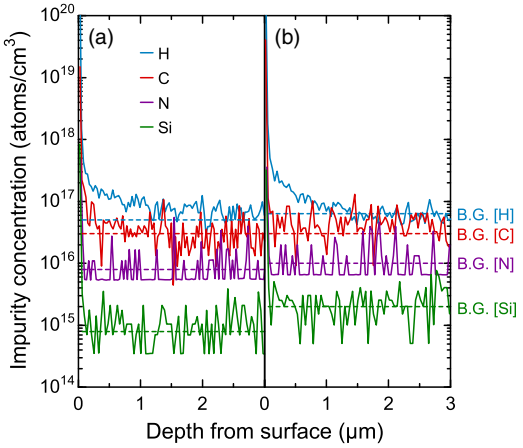

Fig. 5. SIMS depth profiles of impurities in the homoepitaxial layers grown on (010) β-Ga_2O_3 substrates at different TMGa supply rates (growth rates): (a) 1.8×10^2 μmol min^{-1} (5.3 μm h^{-1}) and (b) 5.5×10^2 μmol min^{-1} (16.2 μm h^{-1}). The dashed lines indicate the B.G. levels for each impurity.

between ($\bar{2}$01) heteroepitaxial layers on sapphire substrates and (010) homoepitaxial layers on β-Ga_2O_3 substrates. This result is the same as that obtained by MOVPE using TEGa,[22] but the mechanism is currently unknown.

Figure 4 shows surface NDIC microscopy images, surface AFM images, and XRD {111} pole figures of homoepitaxial layers grown on (010) β-Ga_2O_3 substrates at each TMGa supply rate in Fig. 3. The surface NDIC microscopy images [Figs. 4(a)–4(d)] show that when the TMGa supply rate exceeded 1.8×10^2 μmol min^{-1} (growth rate of 5.3 μm h^{-1}), hillocks extending in the [001] direction developed on the surface. The height of the hillocks increased to $\sim$2 μm at maximum as the growth rate (grown layer thickness) increased; however, their density remained almost constant at $\sim 5 \times 10^4$ cm^{-2} irrespective of the growth rate. Recently, it has been reported that nanopipes present in the substrate are the cause of hillocks formed on the surface of homoepitaxial layers grown on (010) β-Ga_2O_3 substrates.[30] This is thought to be the reason why the hillock density remained constant regardless of the growth rate. However, the AFM images of the areas without hillocks [Figs. 4(e)–4(h)] show that the surface became smoother as the growth rate (grown layer thickness) increased, as indicated by smaller rms roughness (R_{rms}) values. A decrease in the input VI/III ratio with an increase in the TMGa supply rate might also explain the result; however, details should be clarified in future work. In addition, irrespective of the growth rate, the XRD {111} pole figures [Figs. 4(i)–4(l)] show only a (111) peak at $\phi = 126.3°$ and a ($\bar{1}1\bar{1}$) peak at $\phi = 306.3°$ when ψ is 33.0°. The results indicate that homoepitaxial growth of (010) β-Ga_2O_3 single-crystalline layers is possible without the formation of in-plane twins, even at growth rates as high as 16 μm h^{-1}; however, the results also indicate that chemical mechanical polishing of the surface to remove hillocks is critical for these homoepitaxial layers to be used in electronic devices.

Figure 5 shows the SIMS impurity depth profiles for the homoepitaxial layers grown with TMGa supply rates of 1.8×10^2 and 5.5×10^2 μmol min^{-1} (growth rates of 5.3 and 16.2 μm h^{-1}, respectively), as shown in Fig. 4. Irrespective of the growth rate, the concentrations of H, C, N, and Si impurities in the homoepitaxial layers were less than their respective B.G. levels. The origin of the H impurities in the 10^{17} atoms cm^{-3} range near the surface is currently unclear. Therefore, thick, high-purity, single-crystalline β-Ga_2O_3 homoepitaxial layers can be grown at high growth rates by optimizing the growth conditions even when TMGa is used as a precursor. The electrical properties of the grown layer and conductivity control by intentional doping are currently under investigation and will be reported elsewhere.

In summary, the high-speed growth of high-purity, thick β-Ga_2O_3 layers at 1000 °C by low-pressure hot-wall MOVPE was investigated. When TMGa is used as the Ga precursor, a higher input VI/III ratio is required than when TEGa is used; however, the growth of ($\bar{2}$01) β-Ga_2O_3 on the entire surface of a 2 inch diameter (0001) sapphire substrate was found to be possible. By selecting a reactor pressure of 2.4–3.4 kPa and increasing the TMGa supply rate, the growth rate of high-purity β-Ga_2O_3 layers could be increased linearly on both (0001) sapphire and (010) β-Ga_2O_3 substrates, and a high growth rate greater than 16 μm h^{-1} was achieved. Although hillocks were observed on the surface of homoepitaxial layers grown on (010) β-Ga_2O_3 substrates, no twinning was observed at growth rates of 0.9–16.2 μm h^{-1}, demonstrating the strong potential for low-pressure hot-wall MOVPE of β-Ga_2O_3 using TMGa.

Acknowledgments This work was supported by the Ministry of Internal Affairs and Communications (MIC) research and development (JPMI00316).

ORCID iDs Junya Yoshinaga https://orcid.org/0009-0002-5892-0419 Kazutada Ikenaga https://orcid.org/0000-0002-0755-5872 Ken Goto https://orcid.org/0000-0002-3371-0020 Yoshinao Kumagai https://orcid.org/0000-0001-8475-9468

1) H. H. Tippins, Phys. Rev. **140**, A316 (1965).
2) T. Onuma, S. Saito, K. Sasaki, T. Masui, T. Yamaguchi, T. Honda, and M. Higashiwaki, Jpn. J. Appl. Phys. **54**, 112601 (2015).
3) M. Higashiwaki, K. Sasaki, A. Kuramata, T. Masui, and S. Yamakoshi, Appl. Phys. Lett. **100**, 013504 (2012).
4) Z. Xia et al., Appl. Phys. Lett. **115**, 252104 (2019).
5) Z. Galazka et al., J. Cryst. Growth **404**, 184 (2014).
6) A. Kuramata, K. Koshi, S. Watanabe, Y. Yamaoka, T. Masui, and S. Yamakoshi, Jpn. J. Appl. Phys. **55**, 1202A2 (2016).
7) E. Ohba, T. Kobayashi, T. Taishi, and K. Hoshikawa, J. Cryst. Growth **556**, 125990 (2021).
8) K. Sasaki, Q. T. Thieu, D. Wakimoto, Y. Koishikawa, A. Kuramata, and S. Yamakoshi, Appl. Phys. Express **10**, 124201 (2017).
9) Z. Hu, K. Nomoto, W. Li, N. Tanen, K. Sasaki, A. Kuramata, T. Nakamura, D. Jena, and H. G. Xing, IEEE Electron Device Lett. **39**, 869 (2018).
10) M. H. Wong, H. Murakami, Y. Kumagai, and M. Higashiwaki, IEEE Electron Device Lett. **41**, 296 (2020).
11) F. Otsuka, H. Miyamoto, A. Takatsuka, S. Kunori, K. Sasaki, and A. Kuramata, Appl. Phys. Express **15**, 016501 (2022).
12) S. Kumar, H. Murakami, Y. Kumagai, and M. Higashiwaki, Appl. Phys. Express **15**, 054001 (2022).
13) B. Wang, M. Xiao, J. Spencer, Y. Qin, K. Sasaki, M. J. Tadjer, and Y. Zhang, IEEE Electron Device Lett. **44**, 221 (2023).
14) K. Nomura, K. Goto, R. Togashi, H. Murakami, Y. Kumagai, A. Kuramata, S. Yamakoshi, and A. Koukitu, J. Cryst. Growth **405**, 19 (2014).
15) H. Murakami et al., Appl. Phys. Express **8**, 015503 (2015).
16) Q. T. Thieu, D. Wakimoto, Y. Koishikawa, K. Sasaki, K. Goto, K. Konishi, H. Murakami, A. Kuramata, Y. Kumagai, and S. Yamakoshi, Jpn. J. Appl. Phys. **56**, 110310 (2017).
17) M. Baldini, M. Albrecht, A. Fiedler, K. Irmscher, R. Schewski, and G. Wagner, ECS J. Solid State Sci. Technol. **6**, Q3040 (2017).
18) Y. Zhang, F. Alema, A. Mauze, O. S. Koksaldi, R. Miller, A. Osinsky, and J. S. Speck, APL Mater. **7**, 022506 (2019).
19) Z. Feng et al., Phys. Status Solidi RRL **14**, 2000145 (2020).

20) A. Bhattacharyya, P. Ranga, S. Roy, J. Ogle, L. Whittaker-Brooks, and S. Krishnamoorthy, Appl. Phys. Lett. **117**, 142102 (2020).
21) K. Goto, K. Ikenaga, N. Tanaka, M. Ishikawa, H. Machida, and Y. Kumagai, Jpn. J. Appl. Phys. **60**, 045505 (2021).
22) K. Ikenaga, N. Tanaka, T. Nishimura, H. Iino, K. Goto, M. Ishikawa, H. Machida, T. Ueno, and Y. Kumagai, J. Cryst. Growth **582**, 126520 (2022).
23) K. Ikenaga, T. Okuyama, H. Tozato, T. Nishimura, S. Sasaki, K. Goto, M. Ishikawa, Y. Takinami, H. Machida, and Y. Kumagai, Jpn. J. Appl. Phys. **62**, SF1019 (2023).
24) M. Yoshida, H. Watanabe, and F. Uesugi, J. Electrochem. Soc. **132**, 677 (1985).
25) A. J. Green et al., IEEE Electron Device Lett. **38**, 790 (2017).
26) E. Farzana, F. Alema, W. Y. Ho, A. Mauze, T. Itoh, A. Osinsky, and J. S. Speck, Appl. Phys. Lett. **118**, 162109 (2021).
27) A. Bhattacharyya, S. Roy, P. Ranga, C. Peterson, and S. Krishnamoorthy, IEEE Electron Device Lett. **43**, 1637 (2022).
28) G. Seryogin, F. Alema, N. Valente, H. Fu, E. Steinbrunner, A. T. Neal, S. Mou, A. Fine, and A. Osinsky, Appl. Phys. Lett. **117**, 262101 (2020).
29) L. Meng, Z. Feng, A. F. M. A. U. Bhuiyan, and H. Zhao, Cryst. Growth Des. **22**, 3896 (2022).
30) T. Nishikawa, K. Goto, H. Murakami, Y. Kumagai, M. Uemukai, T. Tanikawa, and R. Katayama, Jpn. J. Appl. Phys. **62**, SF1015 (2023).